

Extracellular Matrix Stiffening Induces a Malignant Phenotypic Transition in Breast Epithelial Cells

RYAN S. STOWERS,^{1,3} SHANE C. ALLEN,¹ KARLA SANCHEZ,¹ COURTNEY L. DAVIS,¹ NANCY D. EBELT,²
CARLA VAN DEN BERG,⁴ and LAURA J. SUGGS¹

¹Department of Biomedical Engineering, The University of Texas at Austin, Austin, USA; ²Institute for Cellular and Molecular Biology, The University of Texas at Austin, Austin, USA; ³Department of Mechanical Engineering, Stanford University, Stanford, USA; and ⁴College of Pharmacy, The University of Texas at Austin, Austin, USA

(Received 13 June 2016; accepted 11 October 2016; published online 19 October 2016)

Associate Editor Partha Roy oversaw the review of this article.

Abstract—Tumors are much stiffer than healthy tissue, and progressively stiffen as the cancer develops. Tumor stiffening is largely the result of extracellular matrix (ECM) remodeling, for example, deposition and crosslinking of collagen I. Well established *in vitro* models have demonstrated the influence of the microenvironment in regulating tissue homeostasis, with matrix stiffness being a particularly influential mediator. Non-malignant MCF10A mammary epithelial cells (MECs) lose their epithelial characteristics and become invasive when cultured in stiff microenvironments, leading to the hypothesis that tumor stiffening could contribute directly to disease progression. However, previous studies demonstrating MCF10A invasion have been performed in gels with constant mechanical properties, unlike the dynamically stiffening tumor microenvironment. Here, we employ a temporally stiffening hydrogel platform to demonstrate that matrix stiffening induces invasion from and proliferation in MCF10A mammary acini. After allowing MCF10A acini to form in soft hydrogels for 14 days, the gels were stiffened to the level of a malignant tumor, giving rise to a proliferative and invasive phenotype. Cells were observed to collectively migrate away from mammary acini while maintaining cell–cell contacts. Small molecule inhibition of PI3K and Rac1 pathways was sufficient to significantly reduce the number and size of invasive acini after stiffening. Our results demonstrate that temporal matrix stiffening can induce invasion from mammary acini and supports the notion that tumor stiffening could be implicated in disease progression and metastasis.

Keywords—Matrix stiffening, Hydrogel, Breast epithelium, Mechanotransduction, Invasion.

INTRODUCTION

Tumors are much stiffer than the healthy tissue from which they arise.⁵ For example, the elastic mod-

ulus of normal mammary gland tissue is 100–200 Pa, while malignant mammary tumors have been measured to be as stiff as 1000 to 4000 Pa.^{19,27} The difference in stiffness between tumors and healthy tissue is often great enough to be detected by manual palpation; a commonly employed early screening technique. Tumor stiffness increases over time as the tumor develops, due largely to extracellular matrix remodeling, and the stiffness correlates well with disease progression.³³ However, whether the stiffening process directly contributes to disease progression or is merely a byproduct is still a topic of debate.

While consensus on which molecular mechanisms underlie the effects of stiffening on tumor progression is still being reached, it is widely accepted that the mechanics of the tumor microenvironment has a great influence on disease development.^{25,35} Both healthy and malignant mammary epithelium can be modeled *in vitro* by utilizing hydrogel platforms that recapitulate the essential compositional and mechanical features of the *in vivo* microenvironment. Non-malignant mammary epithelial cells (MECs), such as MCF10A, grown in reconstituted basement membrane extract, commercially available as Matrigel, form multicellular, polarized, hollow spheres known as acini,⁸ which represent the basic functional unit of a healthy mammary gland.²⁵ Conversely, malignant or tumorigenic cells cultured within these gels adopt a range of morphologies from multicellular clusters to invasive masses.¹³ Thus, morphology within Matrigel can generally be used to distinguish normal and malignant phenotypes.²⁹

Using Matrigel as a model system, several seminal papers have identified matrix stiffness as a key contributor to loss of epithelial character and emergence of malignant traits from a normal population of MECs. Matrigel has an elastic modulus of 175 Pa,²⁷

Address correspondence to Laura J. Suggs, Department of Biomedical Engineering, The University of Texas at Austin, Austin, USA. Electronic mail: suggs@utexas.edu

similar to that of normal mammary gland tissue.^{19,27} A layer of Matrigel was overlaid on polyacrylamide gel substrates of variable elastic moduli (150 to 5000 Pa) to generate gels of desired modulus. On soft Matrigel overlays, MCF10A cells formed canonical mammary acini. On stiffer gels, however, the epithelial character was lost and the MCF10As began to resemble malignant cells.²⁷ Similarly, in true 3D gels composed of alginate and Matrigel interpenetrating networks, MCF10A formed acini in soft gels (90 Pa) and adopted malignant and invasive phenotypes in stiffer gels (945 Pa).⁶ While these studies demonstrate the remarkable impact of matrix stiffness in dictating the ultimate morphology and phenotype of single MCF10A cells, they utilized hydrogels with mechanical properties that were constant over time. As static systems, they are inherently incapable of interrogating the effect a temporal stiffening event might have on a developed mammary acinus, which is a more relevant question in the study of cancer progression.

Others have sought to investigate the effects of temporal stiffening on MCF10A acini by utilizing Matrigel-collagen I gels, where stiffening can be induced by glycation of collagen I fibers through the addition of ribose.¹⁹ Stiffening the gels resulted in increased size of the acini, along with luminal filling and loss of organization. However, invasion was not observed unless stiffening was accompanied by activation of oncogenic signaling (ErbB2). A significant limitation of this dynamic system is that the overall increase in elastic modulus was less than 50 Pa, far less than the increase in stiffness during tumor progression [>900 Pa^{19,27}] or in the prior studies utilizing static gel conditions [855 Pa,⁶ ~ 5000 Pa²⁷]. Additionally, the cells may be responding to the alterations in collagen network architecture from glycation. In any case, it is possible that a more substantial increase in stiffness could drive invasion from a mammary acinus without oncogenic signaling, though this question remains unaddressed.

Here, we employ a dynamically tunable hydrogel platform to temporally stiffen the matrix around MCF10A acini. The initial stiffness was tuned to mimic the microenvironment of healthy mammary tissue during acinus development, and stiffened to the level of a malignant tumor after 14 days. We assessed the effects of stiffening on MCF10A morphology, proliferation, and signaling through mechanotransduction pathways. Utilization of temporal stiffening hydrogels will allow for more physiologically relevant hypotheses to be probed and could provide routes to novel signaling pathways for treatment of diseases such as cancer.

MATERIALS AND METHODS

Temporal Stiffening

A detailed presentation of the dynamically tunable stiffening system used here has been previously published.³² Briefly, gold nanorods were synthesized using the seed-mediated growth mechanism in cetyl trimethylammonium bromide (CTAB).²⁶ Gold nanorods were centrifuged twice at $18,000\times g$ for 45 min, then stored in dI water. Liposomes loaded with CaCl_2 and gold nanorods were formed *via* interdigitated fusion.^{1,22} 1,2-dipalmitoyl-sn-glycero-3-phosphocholine (DPPC, Avanti Polar Lipids) dissolved in chloroform was used for the liposome synthesis. Lipid cakes were formed in round bottom flasks by rotary evaporation and desiccated overnight. The lipid cake was hydrated with dI water at 55 °C, sonicated, and interdigitated in 4 M ethanol. Interdigitated lipid sheets were separated *via* centrifugation, and the lipid pellet was incubated with 500 mM CaCl_2 and 5% gold nanorods at 55 °C to produce interdigitated fusion vesicles. The liposomes were centrifuged and washed 5 times to remove all unencapsulated nanorods and calcium. Irradiation of the gold nanorods induces surface plasmon resonance, which results in local heating around the nanorod. The heat generation causes a phase transition at 41 °C in the DPPC bilayer, which allows calcium ions to permeate the bilayer and crosslink the alginate gels.^{2,21} Access to the laser (Laser Lab Inc. 1.4 W, 808 nm) used for all experiments was generously provided by Dr. Stanislav Emelianov.

Cell Culture

Human mammary epithelial cells (MCF10A) were obtained from American Type Culture Collection (ATCC). MCF10A were cultured with DMEM/F12 basal media (Life Technologies) containing 5% horse serum (Life Technologies), 20 ng/mL epidermal growth factor (Peprotech), 0.5 mg/mL hydrocortisone (Sigma), 100 ng/mL cholera toxin (Sigma), 10 $\mu\text{g}/\text{mL}$ insulin (Cell Applications, Inc.), and 1% penicillin-streptomycin (Life Technologies).⁸ Media was changed every 2 days and cells were passaged before reaching confluency.

3D Cell Culture

Assay media was used for all 3D cell cultures. The assay media was composed of DMEM/F12 basal media, 2% horse serum, 5 ng/mL epidermal growth factor, 0.5 mg/mL hydrocortisone, 100 ng/mL cholera toxin, 10 $\mu\text{g}/\text{mL}$ insulin, and 1% penicillin-streptomycin.⁸

Pronova UP MVG sodium alginate (FMC Biopolymer) was dissolved in 300 mM NaCl buffered

with HEPES to 4% w/v. Uniformly crosslinked alginate gels were made using insoluble CaCO_3 as a calcium source, and glucono- δ -lactone (GdL),¹⁵ which hydrolyzes upon dissolution in water to release calcium ions. Gels were made with 5 mM CaCO_3 and 10 mM GdL, and a final alginate concentration of 2%. Liposomes were included at 20% of the volume of the gel. Growth factor reduced Matrigel (Corning) was included at 2.45 mg/mL final concentration. Cells were mixed with the alginate solution prior to gelation to ensure a uniform distribution throughout the gel. Gels were pipetted into chambered coverglasses or well plates and allowed to gel at 37 °C for 30 min. Culture media was then carefully pipetted over the gels and changed every other day.

The gels were irradiated after 14 days in culture. The culture media was removed prior to irradiation and replaced immediately afterward. An 808 nm CW laser was positioned above the well plate or chamber slide and exposed for 1 min.

Phase Contrast Microscopy

A Leica DM IRB microscope was used to capture phase contrast images of the MCF10A acini in 3D gels. Images were taken throughout the time period of culture to ensure proper development of the mammary acini. To quantify the number of protrusive colonies, images were taken at day 17, three days after stiffening. A minimum of 30 acini were imaged from at least 3 biological replicates per experimental condition. Acini were manually identified as invasive if there was a non-continuous curvature of the acinus perimeter with one or more protrusions.^{6,31} Acinus size was determined by tracing the outline of the acinus in ImageJ and determining the area.

Multi-photon and Confocal Microscopy

Multi-photon excitation or confocal laser scanning microscopy was used to image the 3D gels. Multi-photon imaging was performed at 770 nm excitation wavelength with a Spectra Physics Mai Tai pulsed laser source. Confocal samples were excited with both 405 nm and 561 nm lasers. A Prairie View Ultima multi-photon microscopy system with a 20 \times or 40 \times objective, or an Olympus Fluoview FV10i confocal microscope with 60 \times objective was used to capture images. ImageJ was used to convert the image sequences into a Z-projection or 3D projections.

Immunocytochemistry

Antibodies against Ki-67 (Thermo Scientific, RM-9106), laminin (Abcam 14509) and β catenin (BD

Transduction 610154) were purchased. The gels were fixed in 2% paraformaldehyde for 15 min on day 17, 3 days after stiffening. The alginate gel porosity is on the nanometer scale, and substantially limits the diffusion of antibodies. The gels were broken up by gentle pipette mixing to reduce the distance the antibodies must diffuse to reach their antigen. The cells were permeabilized with 0.5% Triton-X-100 in DPBS for 10 min at 4 °C and then rinsed three times with DPBS with glycine for 5 min each. The gels were incubated in a blocking solution of 10% goat serum in DPBS for 1 h. The primary antibody was incubated overnight at 4 °C at a dilution of 1:100 in 10% goat serum. The following day, the gels were rinsed three times with DPBS with 0.1% Triton-X-100 for 20 min. The secondary antibody was diluted 1:1000 in 10% goat serum in DPBS and incubated at room temperature in the dark for 90 min. The gels were rinsed three times in DPBS. DAPI was diluted to 5 $\mu\text{g}/\text{mL}$ in DPBS and incubated with the gels for 15 min. The gels were then rinsed three times with DPBS for 15 min. Finally, the gel suspension was pipetted onto coverslips depressed into petri dishes or glass slides, coverslipped and sealed. The slides were imaged immediately or stored at 4 °C in the dark until imaging.

Small Molecule Inhibition

Small molecule inhibitors of mechanotransduction pathways were added on day 14 after irradiation of the gels. The gels were fixed on day 17 and images of acini were captured. The acini size and number of protrusive colonies was determined as previously described. The specific inhibitors (all from Sigma) used were a FAK inhibitor (PF573228, 5 μM), a ROCK inhibitor (Y27632, 10 μM), a MAPK inhibitor (PD98059, 10 μM), a Rac1 inhibitor (NSC23766, 70 μM), and a PI3K inhibitor (LY294002 20 μM). The inhibitors and concentrations were selected based on previous work.^{6,10,23} To assess viability on day 17, media was removed and replaced with media with 16% CellTiter 96 AQueous One solution. After 4 h, the absorbance at 492 nm was measured. Statistical significance was determined *via* a one-way ANOVA with *post hoc* Tukey analysis.

Quantification of Ki-67 Labeled Nuclei

Acini stained for Ki-67 and DAPI were imaged with a Leica DM 3000B fluorescence microscope. The nuclei positive for Ki-67 and DAPI were analyzed in ImageJ. Briefly, the images were converted to black and white and a watershed algorithm was applied to separate adjacent nuclei. A size threshold for a nucleus was applied and the particles were counted using the

automated feature. The number of Ki-67 positive nuclei was divided by the total number of nuclei labeled with DAPI to give the fraction of proliferating cells.

Statistical Analysis

Data are presented as mean \pm SD. JMP 10 statistics software and GraphPad were used to analyze the data. Statistical significance was determined using either the Student's *t* test for comparisons between two groups, or a one-way ANOVA with *post hoc* Tukey's HSD test for multiple comparisons. *P* values of less than 0.05 were considered significant. Unless otherwise stated, all experiments were conducted with at least 3 biological replicates per condition.

RESULTS AND DISCUSSION

Dynamically Tunable Hydrogels

We have previously published a description of the 3D hydrogel system for dynamically tuning matrix stiffness. Briefly, alginate is used as the principal hydrogel component and mixed with Matrigel (2.45 mg/mL final concentration) to provide adhesive and signaling cues to the developing MCF10A acinus. The stiffness of the gels was temporally modulated by including CaCl₂ and gold nanorod-loaded liposomes within the gels. Irradiation of the gold nanorods with near-infrared light causes surface plasmon resonance and local heating of the lipid bilayer.^{9,34} The liposomes undergo a gel-to-fluid phase transition at 41 °C, resulting in a release of calcium ions into the gel. The released calcium ions form additional crosslinks with the alginate polymer chains, thus increasing the stiffness of the gel. Using this system, control gels that were not irradiated had elastic moduli of 151 Pa (Fig. 1b), similar to normal mammary gland tissue [90–167 Pa^{6,27}] and after laser irradiation, the gels were stiffened to 1074 Pa (Fig. 1b), similar to tumor stiffness,^{19,27} and for some studies, an intermediate stiffness of 561 Pa.

MCF10A Morphology in Stiffening Gels

MCF10A cultured in soft alginate-Matrigel gels for 14 days formed mammary acini (Fig. 2). Similar to Chaudhuri *et al.*, the alginate-Matrigel composites did not impair the formation of acini.⁶ Importantly, alginate-Matrigel composites allow for changes in stiffness without significantly altering the gel pore size or ligand availability.⁶ Alginate does not possess cell adhesive moieties, and thus it provides an inert material by which matrix stiffness can be modulated without

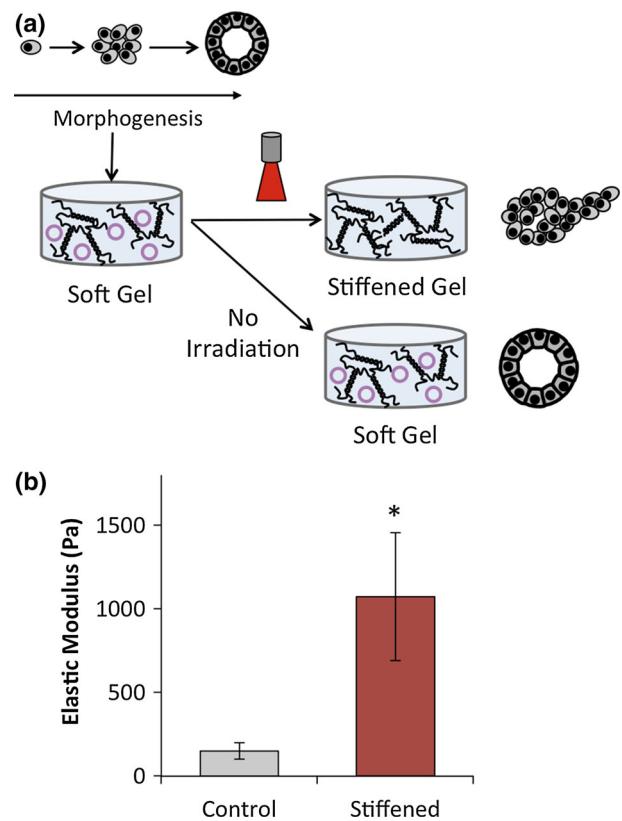


FIGURE 1. (a) Experimental scheme. MCF10A were cultured in alginate-Matrigel composites for 14 days to allow for acinar development. The gels were irradiated to stiffen the matrix around the cells. (b) Elastic modulus of alginate-Matrigel composites increased upon irradiation.

altering other parameters that influence cell-material interactions.^{7,12} Additionally, the presence of liposomes within the gels did not impact acinus development.

Gels were irradiated after 14 days of culture and allowed to grow in stiffened gels for 3 additional days (Fig. 1a). Compared to the spherical acini in control gels, which were soft throughout the experimental timecourse, acini in gels stiffened to tumor-like moduli became invasive (Figs. 3a and 3b). Multicellular protrusions were observed emanating from over half of the acini in stiffened gels (Fig. 3c), while these were rarely seen in acini cultured in soft control gels. Further, the cross-sectional area of acini in stiffened gels was significantly greater than acini in control gels (Fig. 3d). Stiffening to 561 Pa resulted in a moderate increase in the number of invasive acini and acinus area, demonstrating a dose-dependence of the abnormal morphology on stiffening.

The invasive features observed in stiffened gels were multicellular structures that maintained cell-cell contacts, as evidenced by β -catenin expression between neighboring cells (Fig. 4a). This suggests a collective

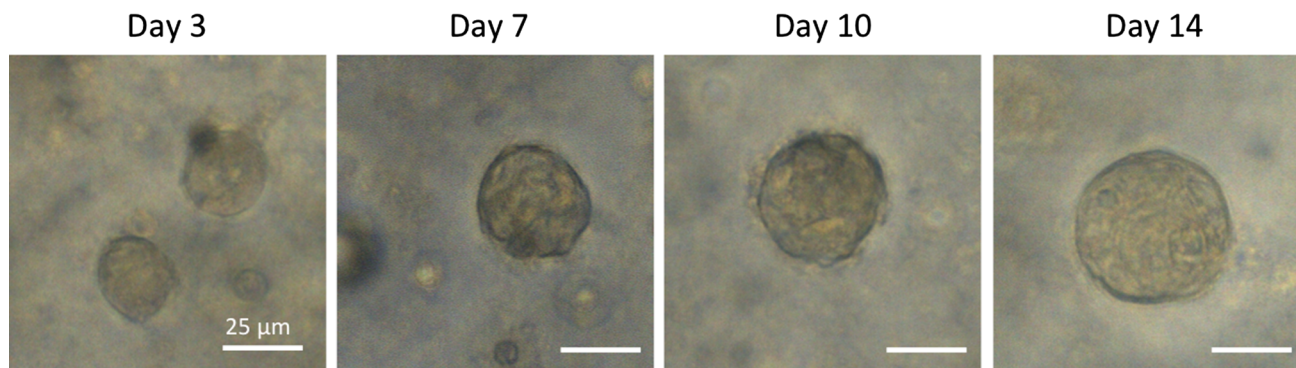


FIGURE 2. Formation of acini from single MCF10A in alginate-Matrigel composite gels over 14 days. Scale bar represents 25 μm .

cell mode of migration, in contrast to single cell dissemination from the acini. Acini in control gels formed a basement membrane, demonstrated by basal laminin staining (Fig. 4b), which became disorganized upon stiffening-induced invasion.

Invasion of MCF10A in static, stiff gels has been previously reported.^{6,27} However, in previous work, single MCF10A cells were seeded within either soft or stiff gels with constant mechanical properties throughout the experiment. Thus, the invasive morphologies observed previously in stiff gels likely did not arise from normal mammary acini. Our results are distinct, in that invasion was induced from a mammary acinus initially formed in a soft microenvironment that was later stiffened. Temporally stiffening the microenvironment around a mature acinus is more physiologically representative of the architectural and microenvironmental changes associated with tumor stiffening and invasion from a previously normal mammary gland.

Levental *et al.* previously sought to determine the effect of temporal stiffening on MCF10A acini.¹⁹ Stiffening was seen to give rise to larger and more disorganized acini, but invasion was not observed without oncogene activation. Notably, the extent of stiffening in the previous work was limited to around 50 Pa, well below that degree of stiffening observed in tumor development and the change in gel stiffness of our study. Thus, it is likely that we observed stiffening-induced invasion without oncogenic activation because of the greater change in stiffness our system provides.

MCF10A Acinus Proliferation After Stiffening

In addition to promoting invasion, stiffening also increased the size of the MCF10A acini (Fig. 3c), suggesting a loss of growth-arrest and an increase in proliferation. This was confirmed by a significant increase in Ki-67 positive nuclei in acini from stiffened gels (Figs. 5a and 5b). While Ki-67 labeled nuclei were

rarely observed in acini from control gels, nearly one-third of nuclei in the stiffened gels were positive for Ki-67. Similarly, MCF10A plated on stiff (6000 Pa) polyacrylamide substrates were increasingly proliferative compared to cells plated on soft substrates.²⁴ Thus, matrix stiffening promotes invasion and proliferation from MCF10A acini, two characteristics typically observed in malignant cell types within 3D gels and tumors *in vivo*, and not typically seen in non-transformed cells like MCF10A.^{3,11,17}

Inhibition of Mechanotransduction Pathways

We sought to determine which mechanotransduction pathways are implicated in promotion of the invasive and proliferative phenotype after stiffening by small molecule inhibition of Rac1, PI3K, MAPK, FAK, and ROCK. Acini treated with Rac1 and PI3K inhibitors showed marked reduction in size and number of invasive colonies compared to untreated, stiffened acini (Figs. 6a and 6b). Less than 30% of acini treated with the PI3K or Rac1 inhibitors were invasive. Both of these groups were significantly lower than untreated cells in stiffened gels, and neither were significantly different from control gels that were not stiffened. The average acinus size in gels treated with either PI3K or Rac1 inhibitors was also significantly lower than the stiffened but untreated acini (Fig. 6b). In addition, the acini treated with the MAPK inhibitor were significantly smaller than untreated acini in stiffened gels, but not less invasive. This points to a possible role for MAPK in promoting proliferation or loss of normal acinus morphology, but not directly in initiation of invasion.

Acini treated with the ROCK and FAK inhibitors showed no change from the untreated acini. However, we cannot draw substantive conclusions about these kinases without further investigation into the efficacy of inhibition in our 3D culture system. Indeed, FAK and ROCK are both implicated in breast cancer pro-

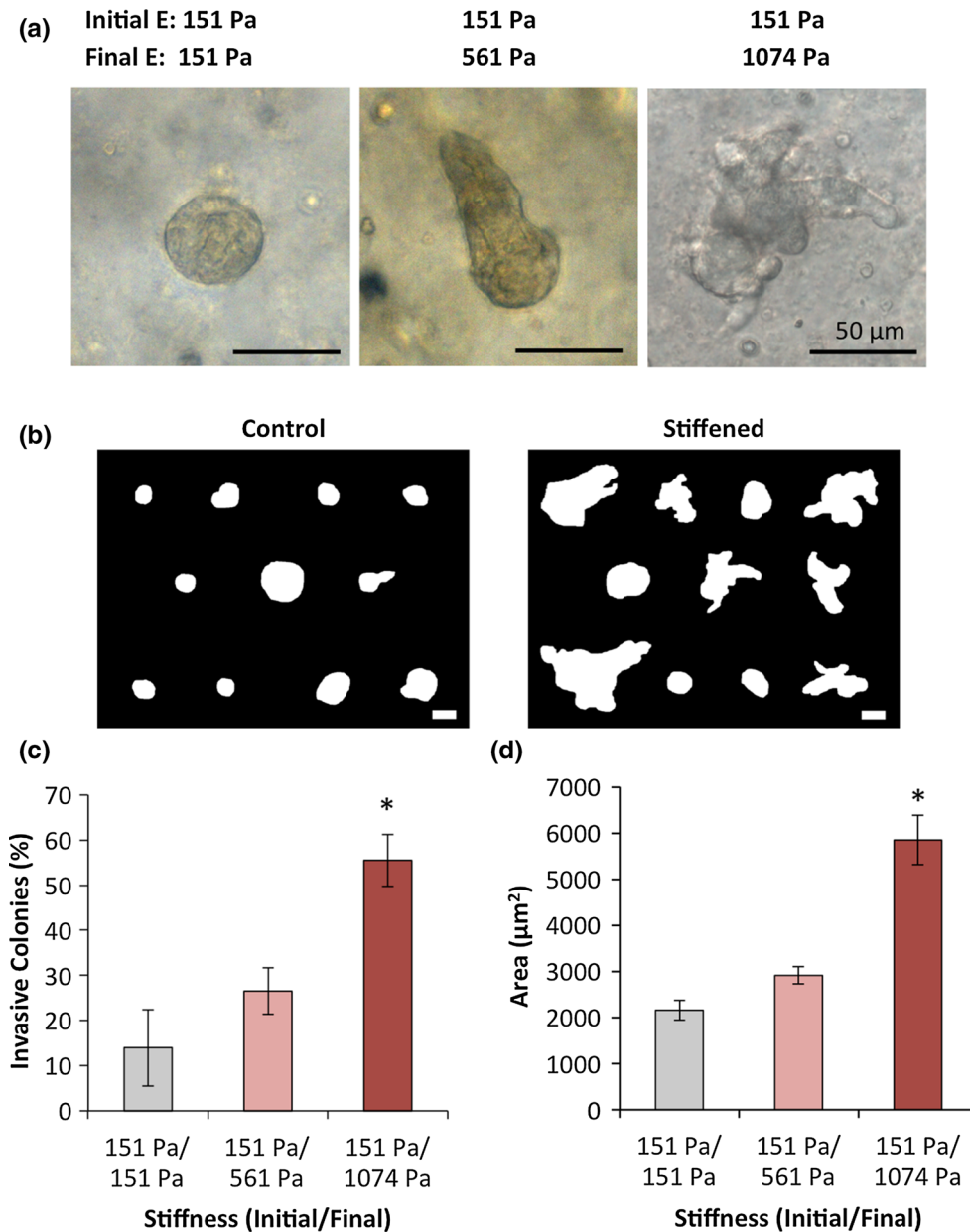


FIGURE 3. Effect of stiffening on MCF10A morphology and phenotype. (a) Morphology of MCF10A after 17 days in culture in static, soft alginate-Matrigel composites (left) and gels that were stiffened on day 14 (middle, right). The invasive phenotype arises after stiffening. Binarized outlines of representative acini in control and stiffened gels, scale bar represents 50 μm . (c) The number of invasive colonies significantly increases upon stiffening to tumor-like stiffness. (d) Acinus area significantly increases with stiffening as well. Error bars for represent s.e.m., * represents $p < 0.05$ compared to control.

gression. Disruption of FAK has been shown to prevent invasion of *in situ* carcinomas in mouse models.¹⁶ ROCK inhibition has been shown to reduce invasion, tumor outgrowth, and bone metastasis of breast cancer cells.^{20,28} Thus, while no significant differences in invasion were observed after small-molecule inhibition of FAK and ROCK in our gel system, both are known to play prime roles in breast cancer mechanotransduction *in vivo*.

Rac1 and PI3K were previously shown to be essential mediators of MCF10A invasion in static, stiff alginate-Matrigel networks.⁶ Inhibition of these molecules led to a reduction in invasion and colony size in stiff gels, similar to our finding that the effects of stiffening were reduced when PI3K or Rac1 was inhibited. Chaudhuri *et al.* suggested that maintenance of a normal phenotype is mediated through clustering of $\beta 4$ integrins. The group

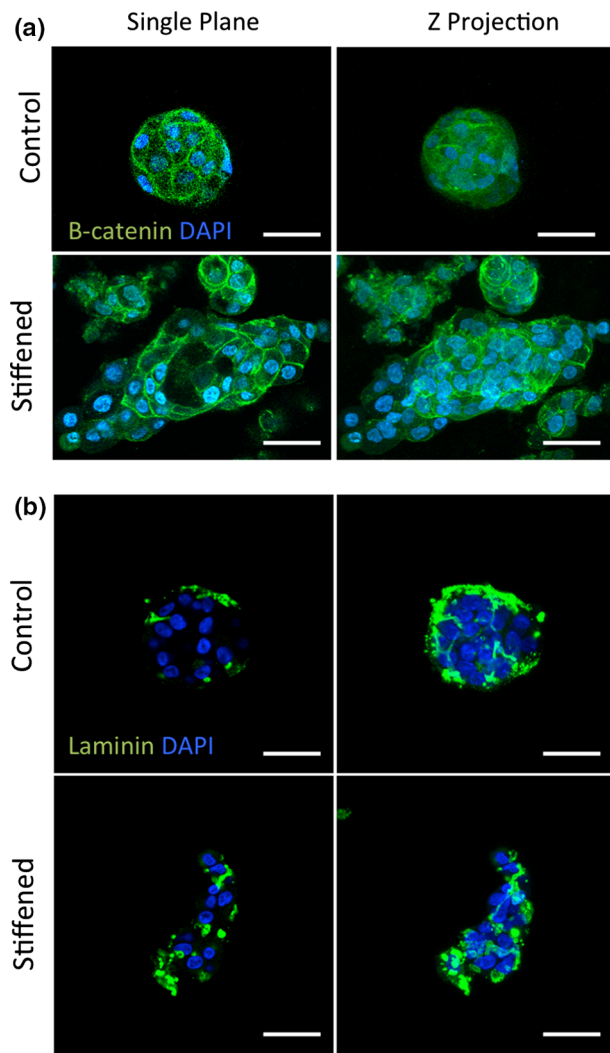


FIGURE 4. Normal acinus polarization is lost upon matrix stiffening expression. (a) Immunofluorescence images of β -catenin (green) and DAPI (blue) for control and stiffened gels. Left column displays a single confocal plane in center of acinus, right column shows a Z projection. (b) Immunofluorescence of laminin (green) and DAPI (blue). Scale bar represents $50\ \mu\text{m}$ in all images.

demonstrated that in stiff gels, the cells were unable to cluster the integrins, leaving the cytoplasmic tails available for phosphorylation by receptor tyrosine kinases, which led to activation of PI3K and Rac1. Our findings, that Rac1 and PI3K inhibition mitigate invasion of MCF10A acini after matrix stiffening, support this proposed model of malignant conversion.

Weaver and colleagues sought to determine the effects of matrix stiffness on multicellular epithelial cell spheroids by transplanting them from soft, reconstituted basement membrane gels to collagen gels of varied stiffness.³⁰ They observed altered morphology, but not invasion, of MCF10A spheroids 48 h after

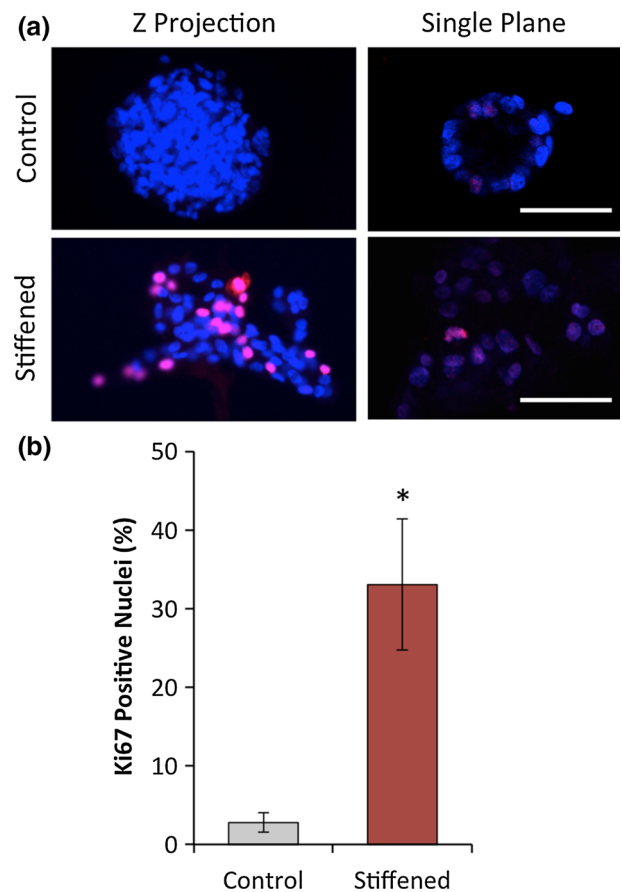


FIGURE 5. Effect of stiffening on MCF10A proliferation in acini. (a) Immunofluorescence of MCF10A nuclei for DAPI and Ki67; Z projections (left) and single confocal planes (right). Scale bar represents $50\ \mu\text{m}$. (b) Quantification of nuclei labeled with Ki67 as a fraction of total nuclei. At least 10 acini (350–700 nuclei) were analyzed for each group.

transplantation to a stiffer (1.5 kPa) collagen gel. Invasion was observed only with H-ras transformed MCF10AT spheroids, and was mediated by PI3K signaling.³⁰ This finding was consistent with previous work from this group that demonstrated invasion occurred only when stiff matrices were coupled with oncogenic signaling.¹⁹ Here, we show a protrusive phenotype arising from a non-transformed population of MCF10A in 3D architectures upon stiffening of the matrix. Interestingly, promotion of the invasive phenotype by matrix stiffening is also driven by the PI3K pathway (Fig. 6).

An invasive phenotype might arise from a mammary acinus by a change in matrix stiffness through several routes. In addition to the signal transduction pathways described above, other intriguing possibilities include alterations in the sensitivity of MCF10A to growth factor signaling and the distribution of mechanical stress in soft and stiffened gels. TGF- β signaling in Madin-Darby canine kidney (MDCK)

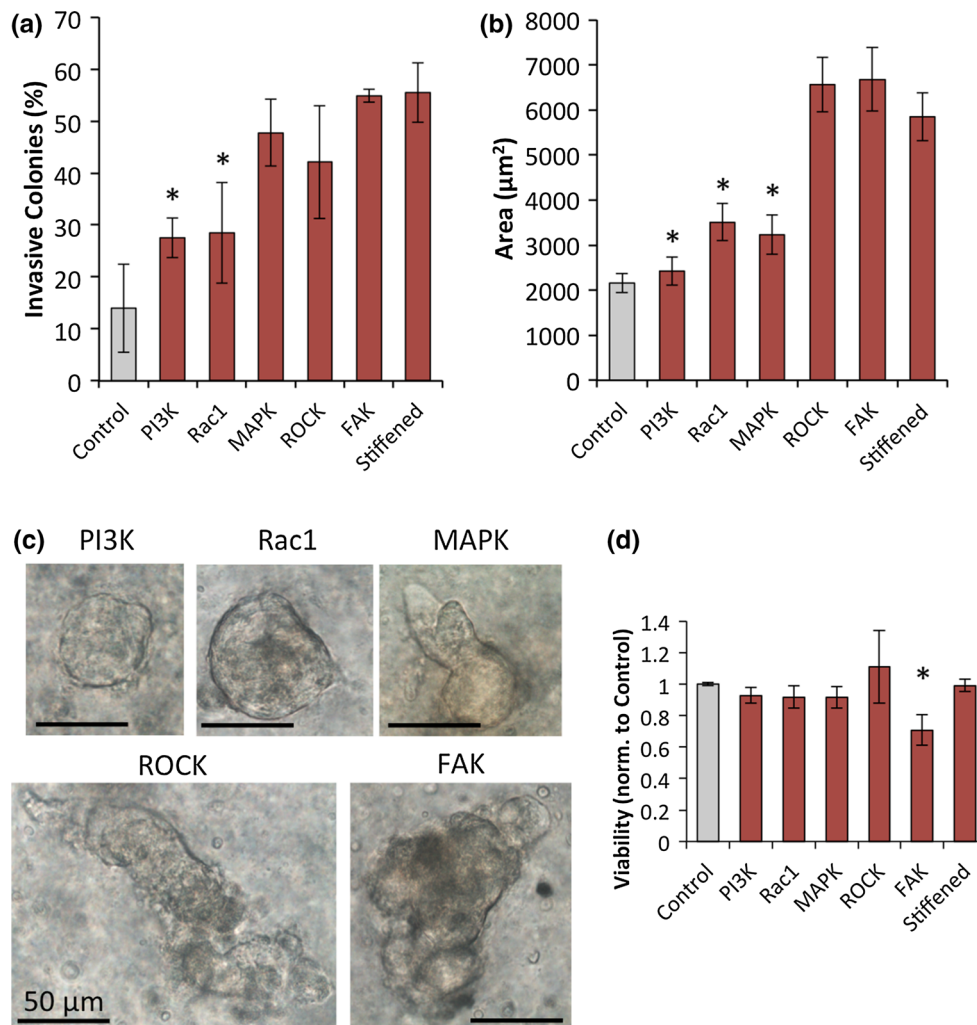


FIGURE 6. Effect of small molecule inhibitors on MCF10A after stiffening. (a) The percentage of invasive acini after treatment with inhibitors of PI3K, Rac1, MAPK, ROCK, and FAK, or stiffened with no treatment, or in statically soft control gels. (b) Acinus area in gels that were stiffened and treated with small molecule inhibitors. Error bars represent s.e.m. (c) Morphology of MCF10A after stiffening and treatment with inhibitors. Inhibition of PI3K and Rac1 yielded smaller, less invasive acini. Treatment with MAPK resulted in smaller acini that were still invasive, while ROCK and FAK treatment produced no discernable effect. (d) Viability was assessed after small molecule inhibition with the MTS assay. FAK was observed to significantly decrease viability compared to the control. All other inhibitors were statistically similar to the control.

epithelial cells depends greatly on the stiffness of the substrate on which the cells are cultured. On compliant substrates, TGF- β induces apoptosis, while on stiff substrates, TGF- β promotes EMT.¹⁸ Additionally, Kim and Asthagiri showed MDCK cells are 100-fold more sensitive to EGF on stiffer substrates than on compliant substrates.¹⁴ On stiff substrates, even EGF doses as low as 0.1 ng/mL caused significant increases in proliferation of the cell clusters. It is possible that similar mechanical switches exist in MCF10A acini in 3D gels, where an increase in matrix stiffness can cause an increase in sensitivity or a change in response to particular cytokines.

The distribution of stress throughout mammary ducts has also been implicated in driving invasion. Using micropatterned acini, Boghaert *et al.* placed a single tumor cell in acini of non-transformed cells at areas of high or low mechanical stress.⁴ The cells in regions of high stress were much more invasive than cells in areas of low stress, despite having similar cell-cell contacts. Overall, the distribution of stress was shown to dictate whether cells invade or remain in the duct. Similarly, a change in matrix stiffness in the system presented here could change the overall stress in a mammary acinus, as cells are able to exert higher traction forces against stiffer matrices. Areas where

stress is concentrated may prime cells for protrusion into the matrix.

CONCLUSION

We have employed a dynamically stiffening 3D hydrogel culture system to model the ECM stiffening that occurs during tumor development, and to assess the impact of stiffening on a mammary epithelium model. We demonstrate that stiffening to a tumor-like level gives rise to invasive and proliferative phenotypes from MCF10A, which were previously in a growth-arrested, quiescent state. We also determined that this phenotypic transition upon stiffening is mediated by the PI3K/Rac1 pathway. This work demonstrates the power of temporal recapitulation of physiological conditions using 3D hydrogel models, and highlights the need for more platforms with dynamically tunable features.

ACKNOWLEDGMENTS

The authors thank S. Emelianov for access to the laser, A. Brock for kindly providing the laminin antibody, and K. Wisdom for reviewing the manuscript. This work was supported by the Cancer Prevention and Research Institute of Texas (RP130372).

CONFLICT OF INTEREST

Ryan S. Stowers, Shane C. Allen, Karla Sanchez, Courtney L. Davis, Nancy D. Ebelt, Carla Van Den Berg, and Laura J. Suggs declare no conflicts of interest.

ETHICAL STANDARDS

No human or animal studies were carried out by the authors for this article.

REFERENCES

- ¹Ahl, P. L., L. Chen, W. R. Perkins, S. R. Minchey, L. T. Boni, T. F. Taraschi, *et al.* Interdigitation-fusion: a new method for producing lipid vesicles of high internal volume. *Biochim. Biophys. Acta* 1195:237–244, 1994.
- ²Andersen, T., A. Kyrsting, and P. M. Bendix. Local and transient permeation events are associated with local melting of giant liposomes. *Soft Matter* 10:4268–4274, 2014.
- ³Bissell, M. J., and D. Radisky. Putting tumours in context. *Nat. Rev. Cancer* 1:46–54, 2001.
- ⁴Boghaert, E., J. P. Gleghorn, K. Lee, N. Gjorevski, D. Radisky, and C. M. Nelson. Host epithelial geometry regulates breast cancer cell invasiveness. *Proc. Natl Acad. Sci. U S A* 109:19632–19637, 2012.
- ⁵Butcher, D. T., T. Alliston, and V. M. Weaver. A tense situation: forcing tumour progression. *Nat. Rev. Cancer* 9:108–122, 2009.
- ⁶Chaudhuri, O., S. T. Koshy, C. Branco da Cunha, J. W. Shin, C. S. Verbeke, K. H. Allison, *et al.* Extracellular matrix stiffness and composition jointly regulate the induction of malignant phenotypes in mammary epithelium. *Nat. Mater.* 13:970–978, 2014.
- ⁷da Cunha, C. B., D. D. Klumpers, W. A. Li, S. T. Koshy, J. C. Weaver, O. Chaudhuri, *et al.* Influence of the stiffness of three-dimensional alginate/collagen-I interpenetrating networks on fibroblast biology. *Biomaterials* 35:8927–8936, 2014.
- ⁸Debnath, J., S. K. Muthuswamy, and J. S. Brugge. Morphogenesis and oncogenesis of MCF-10A mammary epithelial acini grown in three-dimensional basement membrane cultures. *Methods* 30:256–268, 2003.
- ⁹Eustis, S., and M. A. El-Sayed. Why gold nanoparticles are more precious than pretty gold: noble metal surface plasmon resonance and its enhancement of the radiative and nonradiative properties of nanocrystals of different shapes. *Chem. Soc. Rev.* 35:209–217, 2006.
- ¹⁰Guo, C. L., M. Ouyang, J. Y. Yu, J. Maslov, A. Price, and C. Y. Shen. Long-range mechanical force enables self-assembly of epithelial tubular patterns. *Proc. Natl Acad. Sci. U S A* 109:5576–5582, 2012.
- ¹¹Hanahan, D., and R. A. Weinberg. Hallmarks of cancer: the next generation. *Cell* 144:646–674, 2011.
- ¹²Huebsch, N., P. R. Arany, A. S. Mao, D. Shvartsman, O. A. Ali, S. A. Bencherif, *et al.* Harnessing traction-mediated manipulation of the cell/matrix interface to control stem-cell fate. *Nat Mater* 9:518–526, 2010.
- ¹³Kenny, P. A., G. Y. Lee, C. A. Myers, R. M. Neve, J. R. Semeiks, P. T. Spellman, *et al.* The morphologies of breast cancer cell lines in three-dimensional assays correlate with their profiles of gene expression. *Mol. Oncol.* 1:84–96, 2007.
- ¹⁴Kim, J. H., and A. R. Asthagiri. Matrix stiffening sensitizes epithelial cells to EGF and enables the loss of contact inhibition of proliferation. *J. Cell Sci.* 124:1280–1287, 2011.
- ¹⁵Kuo, C. K., and P. X. Ma. Maintaining dimensions and mechanical properties of ionically crosslinked alginate hydrogel scaffolds in vitro. *J. Biomed. Mater. Res. A* 84:899–907, 2008.
- ¹⁶Lahlou, H., V. Sanguin-Gendreau, M. C. Frame, and W. J. Muller. Focal adhesion kinase contributes to proliferative potential of ErbB2 mammary tumour cells but is dispensable for ErbB2 mammary tumour induction in vivo. *Breast Cancer Res.* 14:R36, 2012.
- ¹⁷Lee, G. Y., P. A. Kenny, E. H. Lee, and M. J. Bissell. Three-dimensional culture models of normal and malignant breast epithelial cells. *Nat. Methods* 4:359–365, 2007.
- ¹⁸Leight, J. L., M. A. Wozniak, S. Chen, M. L. Lynch, and C. S. Chen. Matrix rigidity regulates a switch between TGF- β 1-induced apoptosis and epithelial-mesenchymal transition. *Mol. Biol. Cell* 23:781–791, 2012.
- ¹⁹Levental, K. R., H. Yu, L. Kass, J. N. Lakins, M. Egeblad, J. T. Erler, *et al.* Matrix crosslinking forces tumor progression by enhancing integrin signaling. *Cell* 139:891–906, 2009.
- ²⁰Liu, S., R. H. Goldstein, E. M. Scepansky, and M. Rosenblatt. Inhibition of rho-associated kinase signaling

- prevents breast cancer metastasis to human bone. *Cancer Res.* 69:8742–8751, 2009.
- ²¹Messersmith, P. B., and S. Starke. Thermally triggered calcium phosphate formation from calcium-loaded liposomes. *Chem. Mater.* 10:117–124, 1998.
- ²²Messersmith, P. B., S. Vallabhaneni, and V. Nguyen. Preparation of calcium-loaded liposomes and their use in calcium phosphate formation. *Chem. Mater.* 10:109–116, 1998.
- ²³Muranen, T., L. M. Selfors, D. T. Worster, M. P. Iwanicki, L. Song, F. C. Morales, *et al.* Inhibition of PI3K/mTOR leads to adaptive resistance in matrix-attached cancer cells. *Cancer Cell* 21:227–239, 2012.
- ²⁴N. Physical Sciences–Oncology Centers, D. B. Agus, J. F. Alexander, W. Arap, S. Ashili, and J. E. Aslan, *et al.*, A physical sciences network characterization of non-tumorigenic and metastatic cells. *Sci. Rep.* 3: 1449, 2013.
- ²⁵Nelson, C. M., and M. J. Bissell. Modeling dynamic reciprocity: engineering three-dimensional culture models of breast architecture, function, and neoplastic transformation. *Semin. Cancer Biol.* 15:342–352, 2005.
- ²⁶Nikoobakht, B., and M. A. El-Sayed. Preparation and growth mechanism of gold nanorods (NRs) using seed-mediated growth method. *Chem. Mater.* 15:1957–1962, 2003.
- ²⁷Paszek, M. J., N. Zahir, K. R. Johnson, J. N. Lakins, G. I. Rozenberg, A. Gefen, *et al.* Tensional homeostasis and the malignant phenotype. *Cancer Cell* 8:241–254, 2005.
- ²⁸Patel, R. A., K. D. Forinash, R. Pireddu, Y. Sun, N. Sun, M. P. Martin, *et al.* RKI-1447 is a potent inhibitor of the Rho-associated ROCK kinases with anti-invasive and antitumor activities in breast cancer. *Cancer Res.* 72:5025–5034, 2012.
- ²⁹Petersen, O. W., L. Ronnov-Jessen, A. R. Howlett, and M. J. Bissell. Interaction with basement membrane serves to rapidly distinguish growth and differentiation pattern of normal and malignant human breast epithelial cells. *Proc. Natl Acad. Sci. U S A* 89:9064–9068, 1992.
- ³⁰Rubashkin, M. G., L. Cassereau, R. Bainer, C. C. DuFort, Y. Yui, G. Ou, *et al.* Force engages vinculin and promotes tumor progression by enhancing PI3K activation of phosphatidylinositol (3, 4, 5)-triphosphate. *Cancer Res.* 74:4597–4611, 2014.
- ³¹Shi, Q., R. P. Ghosh, H. Engelke, C. H. Rycroft, L. Cassereau, J. A. Sethian, *et al.* Rapid disorganization of mechanically interacting systems of mammary acini. *Proc. Natl Acad. Sci. U S A* 111:658–663, 2014.
- ³²Stowers, R. S., S. C. Allen, and L. J. Suggs. Dynamic phototuning of 3D hydrogel stiffness. *Proc. Natl Acad. Sci. U S A* 112:1953–1958, 2015.
- ³³Wirtz, D., K. Konstantopoulos, and P. C. Searson. The physics of cancer: the role of physical interactions and mechanical forces in metastasis. *Nat. Rev. Cancer* 11:512–522, 2011.
- ³⁴Wu, G., A. Mikhailovsky, H. A. Khant, C. Fu, W. Chiu, and J. A. Zasadzinski. Remotely triggered liposome release by near-infrared light absorption via hollow gold nanoshells. *J. Am. Chem. Soc.* 130:8175–8177, 2008.
- ³⁵Yu, H., J. K. Mouw, and V. M. Weaver. Forcing form and function: biomechanical regulation of tumor evolution. *Trends Cell Biol.* 21:47–56, 2011.